For publication in the International Journal of Heat & Mass Transfer

APPROXIMATE PREDICTIONS OF THE TRANSPORT OF THERMAL RADIATION THROUGH AN ABSORBING PLANE LAYER

42p

Submitted for Publication

[1963] 42p refs

51097

NASA TM X [redacted]

By Max. A. Heaslet and Franklyn B. Fuller

National Aeronautics and Space Administration
Ames Research Center
Moffett Field, Calif.

~~X 64 10273~~ A

N65-88953

Code 2A

(NASA TM X-51097)

10273

ABSTRACT

The transport of thermal radiation through an absorbing medium bounded by parallel walls is predicted. The walls are heated and are assumed to emit, reflect, and transmit the radiation isotropically. The medium is assumed to be in local thermodynamic equilibrium and to have radiative characteristics that can be averaged over the entire frequency range. First, relations are given whereby the solution becomes available once the problem associated with the case of opaque, black walls is solved. Second, different methods are employed to derive approximations of radiative flux and temperature distribution through the medium. Simple formulas, of interest in engineering design and analysis, appear as a by-product of the study. Comparisons are made with previously published numerical results. AUTHOR

INTRODUCTION

A number of references are now available in which the equations characterizing the transport of thermal radiation through an absorbing medium are formulated and mathematical techniques leading to actual predictions are developed. Foremost among these are the treatises of

Chandrasekhar [1], Kourganoff [2], and Sobolev [3]. The analysis retains considerable algebraic complexity, however, partially because of the multiplicity of physical parameters affecting the phenomena and the number of additional idealizations that are of practical interest. Thus, in spite of the theoretical understanding that has been achieved, and although numerical solutions by means of high-speed computers offer no essential difficulties, the problem of efficient presentation of results remains a challenge. The present paper attempts to contribute some efficiency of presentation to predictions of radiative transport through an absorbing medium contained between two parallel walls with specified temperatures and known radiative characteristics.

Two parallel objectives are to be kept in mind. First, a close connection is established between the general problem of radiative energy transport between walls that emit, transmit, and reflect isotropically and the problem of transport between opaque, black walls. The latter case has been treated by Usiskin and Sparrow [4] and numerical solutions have been given for different values of the optical thickness of the plane layer between the walls. It will be shown here that the results of [4] may be applied with only minor modification to the more general case. Second, since the calculations of Usiskin and Sparrow are available for comparison, approximations to the solutions of the governing equations are studied. In this way, rather simple expressions are derived that provide a surprising accuracy and that certainly should be useful in preliminary design or engineering analysis.

In the next section the governing equations are derived. The more or less conventional approach leads to an expression for flux of radiation that was given explicitly by R. and M. Goulard [5]. Differences in terminology were considered necessary and the derivation of wall conditions was cast in a different form, all of which prompted the inclusion of this basic material. The discussion of the general solution gives a proof that iterative methods can be used to solve the basic integral equation and then relates the problem to the case of black walls. The remaining portion of the paper deals with approximations and comparisons between solutions involving differing orders of accuracy.

Three methods, yielding increasing degrees of accuracy, will evolve. The first, based on the use of an exponential influence function in place of the exact exponential-integral function, simplifies the analysis so much that all results can be expressed algebraically. The detailed distribution of the temperature (or the emission) within the medium suffers increasing inaccuracy near the walls but further integration to determine flux between the walls leads to predictions that are never in error more than a few percent. Perhaps more important is the fact that the formulas are easily manipulated to display major effects of variations in the various physical parameters. The second method is similar in approach to the Milne-Eddington approximation used in the study of stellar atmospheres and improves the accuracy of the predictions without introducing undue complexity. Finally, an iterative calculation of a particularly simple form provides estimates that agree well with the more accurate numerical solutions that are available. These iterative calculations are then used to establish the degree of confidence one can have in the other approximations.

TABLE OF SYMBOLS

A	$(1/2)[(1/2) - E_3(\xi_L)]$
B_ν	Planck's function (see eq. (5))
$E_n(x)$	integroexponential function of order n; $E_n(x) = \int_1^\infty e^{-xt}t^{-n}\,dt$
$H(\xi,\xi_L)$	integral used in iterative solution (see eq. (48b))
$I(x,\mu)$	specific intensity, energy per unit area, time, solid angle
j	local emission coefficient, per unit mass
J	source function (see eq. (5))
K_0, K_1	weighted integrals of emission function (see eqs. (27) and (32b))
L	geometric thickness of plane layer (fig. 1)
m, n	coefficients used in exponential approximation of $E_2(x)$ (see eq. (35))
q	rate of energy transport per unit area
r	reflectivity
t	transmissivity
T	temperature, absolute
x	geometric depth in absorbing layer
Z	see equations (27)
α	absorptivity

$\beta(\xi)$	emission function (see eq. (11))
γ	coefficient of cubic term in approximation of emission function (see eq. (46))
Δ	see equation (29)
ϵ	emissivity
θ	angle between ray and element normal to surface (see fig. 1)
κ	local absorption coefficient, per unit mass
λ	slope of linear approximation to emission function (see eq. (45a))
μ	$\cos\theta$
ξ	optical depth in absorbing layer ($d\xi = \rho\kappa\, dx$)
ρ	local density of absorbing medium
σ	Stefan's constant
$\varphi(\xi)$	dimensionless form of emission function (see eq. (25))

Subscripts

o	evaluated at $\xi = 0$
L	evaluated at $\xi = \xi_L = \int_0^L \rho\kappa\, dx$

Superscripts

+	right-going (ξ increasing) quantity
-	left-going (ξ decreasing) quantity

GOVERNING EQUATIONS

Figure 1 shows the orientation of the coordinate system to be used. The two walls are situated at $x = 0$ and $x = L$. Let conditions at either wall be indicated by the subscript i where $i = 0$ or L. Then, we have temperature, T_i, emissivity, ϵ_i, absorptivity, α_i, reflectivity, r_i, and transmissivity, t_i, prescribed as known boundary conditions where

$$\alpha_i = \epsilon_i \tag{1a}$$

$$\alpha_i + t_i + r_i = 1 \tag{1b}$$

It is assumed that the gas and walls have characteristics that may be averaged over the entire frequency range of the radiation, so that a <u>gray</u> analysis applies, and the walls emit and reflect diffusely.

The basic equation of radiative transfer is (see, e.g., [2])

$$\mu \frac{dI(x,\mu)}{dx} = -\rho\kappa I(x,\mu) + \rho j \tag{2}$$

Equation (2) is preferably expressed in terms of the independent variable ξ (optical depth) where

$$d\xi = \rho\kappa \; dx \tag{3}$$

and thus becomes

$$\mu \frac{dI}{d\xi} + I = J \tag{4}$$

where J $(=j/\rho\kappa)$ is called the source function. Provided the refractive index of the medium is 1 and local thermodynamic equilibrium is achieved, the source function is given by

$$J = \int_0^\infty B_\nu \, d\nu = \frac{\sigma}{\pi} T^4 \tag{5}$$

where

$$B_\nu \left(= \frac{2h\nu^3}{c^2} \frac{\exp(-h\nu/kT)}{1 - \exp(-h\nu/kT)} \right) \qquad \text{Planck's function}$$

ν	frequency
h,k,σ	Planck, Boltzmann, and Stefan constants
c	velocity of light

The notation

$$\left.\begin{aligned} I &= I^+(\xi,\mu) \qquad 0 \le \mu \le 1 \\ &= I^-(\xi,\mu) \qquad -1 \le \mu \le 0 \end{aligned}\right\} \tag{6}$$

serves to distinguish the rate of flow of energy per unit area and solid angle for positive and negative values of $\mu(=\cos\,\theta)$. With this notation, the solution of equation (4) in the two regimes becomes

$$I^+(\xi,\mu) = I^+(0)\exp(-\xi/\mu) + \int_0^\xi J(\xi_1)\exp[-(\xi - \xi_1)/\mu](d\xi_1/\mu) \tag{7a}$$

$$I^-(\xi,\mu) = I^-(\xi_L)\exp[-(\xi - \xi_L)/\mu] + \int_\xi^{\xi_L} J(\xi_1)\exp[-(\xi - \xi_1)/\mu](d\xi_1/-\mu) \tag{7b}$$

where $I^+(0)$ and $I^-(\xi_L)$ are the isotropic specific intensities induced by the walls at $\xi = 0$ and $\xi_L = \int_0^L \rho\kappa \, dx$, respectively.

The total rates of energy transport per unit area in the positive and negative x directions are

$$q^+(\xi) = 2\pi \int_0^1 I^+(\xi,\mu)\mu \, d\mu \tag{8a}$$

$$q^-(\xi) = 2\pi \int_0^{-1} I^-(\xi,\mu)\mu \, d\mu \tag{8b}$$

The values of $q^+(\xi)$ and $q^-(\xi)$ are sometimes referred to as the right and left fluxes of radiation. Equations (7) and (8) yield the two relations

$$q^+(\xi) = 2q_0^+ E_3(\xi) + 2\pi \int_0^{\xi} J(\xi_1)E_2(\xi - \xi_1)d\xi_1 \tag{9a}$$

$$q^-(\xi) = 2q_L^- E_3(\xi_L - \xi) + 2\pi \int_{\xi}^{\xi_L} J(\xi_1)E_2(\xi_1 - \xi)d\xi_1 \tag{9b}$$

where $q_0^+ = \pi I^+(0)$, $q_L^- = \pi I^-(\xi_L)$ and $E_n(\xi)$ is the nth exponential integral defined as

$$E_n(\xi) = \int_0^1 e^{-\xi/\mu} \mu^{n-2} \, d\mu = \int_1^{\infty} \frac{e^{-\xi x}}{x^n} dx$$

If local unidimensional energy flux (net energy transport per unit time and area) is denoted $q(\xi)$, one has

$$q(\xi) = q^+(\xi) - q^-(\xi) \tag{10}$$

and $q(\xi) > 0$ obviously corresponds to a net energy flow in the positive x direction. From equations (9) and (10) follows the fundamental relation. After setting

$$\pi J(\xi) = \beta(\xi) = \sigma T^4(\xi) \tag{11}$$

one gets

$$q(\xi) = 2q_0^+ E_3(\xi) - 2q_L^- E_3(\xi_L - \xi) + 2\int_0^{\xi_L} \beta(\xi_1)\operatorname{sgn}(\xi - \xi_1)E_2(|\xi - \xi_1|)d\xi_1 \tag{12}$$

It will be noted that the expression $\operatorname{sgn}(\xi - \xi_1)E_2(|\xi - \xi_1|)$, in the integrand of (12), is discontinuous when $\xi_1 = \xi$. This requires care in differentiation.

Equation (12) is the flux equation for our unidimensional problem. The notation does not agree precisely with conventional astrophysical terminology but the choice of variables should preclude any ambiguities. The value of $q(\xi)$ differs by a factor π from the astrophysicists' flux, usually denoted F. Sign conventions are also changed. The independent variable ξ is, of course, dimensionless since the volumetric absorption coefficient $\rho\kappa$ is measured in terms of the reciprocal of radiation mean free path length.

The dimensionless parameter ξ_L (optical thickness of layer) will be seen later to play a unique role in fixing the nature of the variation of the emission function $\beta(\xi)$. It should be remarked that in some references the volumetric absorption coefficient is assumed a constant so that ξ_L becomes $\rho\kappa L$. The transformation to optical path length in equation (3) shows that this restriction is not necessary. In a recent paper, Probstein [6] has developed an analogy between $\rho\kappa L$ and the inverse Knudsen number of low-density fluid mechanics. The Knudsen number appears in molecular transport phenomena and is the ratio of molecular collision mean free path to the characteristic flow length. The term $\rho\kappa L$ can similarly be expressed as the ratio between characteristic length and the mean free path of a photon. This concept is of considerable heuristic value and enables Probstein to present, for the case of black walls, an approximate expression for flux by means of the analogy. Similar approximate results that apply to more arbitrary wall conditions will be considered in the final section of this paper.

Calculation of Input Conditions at Walls

The magnitudes of q_o^+ and q_L^- are related to the wall temperatures (or direct wall emission) as well as the wall parameters introduced in equations (1). Two equalities exist which serve to fix these values. Thus, one can write the two balances

$$q_o^+ = \epsilon_o \sigma T_o{}^4 + r_o q_o^- \tag{13a}$$

$$q_L^- = \epsilon_L \sigma T_L{}^4 + r_L q_L^+ \tag{13b}$$

These relations simply state that the energy per unit time and area coming from each of the walls is equal to the direct emission plus the reflected portion of the incoming radiation from external sources, that is, from the other wall and the medium between the walls. The quantitative expressions for q_o^- and q_L^+ are, from equations (9),

$$q_o^- = 2q_L^- E_3(\xi_L) + 2\int_o^{\xi_L} \beta(\xi_1)E_2(\xi_1)d\xi_1$$

$$q_L^+ = 2q_o^+ E_3(\xi_L) + 2\int_o^{\xi_L} \beta(\xi_1)E_2(\xi_L - \xi_1)d\xi_1$$

From equations (13) the desired conditions at the walls now follow; thus

$$q_o^+ = [1 - 4r_or_LE_3^2(\xi_L)]^{-1}\left[\epsilon_o\sigma T_o^4 + 2r_o\epsilon_LE_3(\xi_L)\sigma T_L^4 + 2r_o\int_o^{\xi_L} \beta(\xi_1)E_2(\xi_1)d\xi_1 + 4r_or_LE_3(\xi_L)\int_o^{\xi_L} \beta(\xi_1)E_2(\xi_L - \xi_1)d\xi_1\right] \tag{14a}$$

$$q_L^- = [1 - 4r_or_LE_3^2(\xi_L)]^{-1}\left[2r_L\epsilon_oE_3(\xi_L)\sigma T_o^4 + \epsilon_L\sigma T_L^4 + 2r_L\int_o^{\xi_L} \beta(\xi_1)E_2(\xi_L - \xi_1)d\xi_1 + 4r_or_LE_3(\xi_L)\int_o^{\xi_L} \beta(\xi_1)E_2(\xi_1)d\xi_1\right] \tag{14b}$$

Basic Integral Equation for Constant Flux

For constant wall temperatures and local thermodynamic equilibrium, $q(\xi)$, as given in equation (12), must be a constant. The derivative of $q(\xi)$, from equation (12), is

$$\frac{dq}{d\xi} = -2q_o^+ E_2(\xi) - 2q_L^- E_2(\xi_L - \xi) + 4\beta(\xi) - 2\int_o^{\xi_L} \beta(\xi_1)E_1(|\xi - \xi_1|)d\xi_1 \tag{15}$$

and for constant flux one gets the basic integral equation

$$\beta(\xi) = \frac{1}{2}\, q_0^+ \, E_2(\xi) + \frac{1}{2}\, q_L^- \, E_2(\xi_L - \xi) + \frac{1}{2}\int_0^{\xi_L} \beta(\xi_1) E_1(|\xi - \xi_1|)\, d\xi_1 \tag{16}$$

Two special cases of equation (16) are of particular interest. First, for opaque, black walls, $t_1 = 0$, $r_1 = 0$, and the wall emissions, as given in equations (14), are

$$q_0^+ = \sigma T_0^{\,4}\ , \qquad q_L^- = \sigma T_L^{\,4}$$

Usiskin and Sparrow [4] have given numerical results corresponding to these conditions. The importance of this case is enhanced once one observes in equations (14) that q_0^+ and q_L^- have no explicit dependence on ξ and that the analysis can proceed formally without a precise stipulation concerning physical conditions at the walls. Equation (16) is thus used to determine solutions in terms of the parameters q_0^+ and q_L^- and the connection between these parameters and the actual boundary conditions is established later in an auxiliary calculation.

A second case of interest arises in relating equation (16) to the problem of a plane, parallel, semi-infinite stellar atmosphere. This idealization occurs when the left wall at $x = 0$ is transparent ($t_0 = 1$, $r_0 = 0$) and the right wall is allowed to recede to an infinite distance. Here, the driving terms in the right member of equation (16) vanish, since $q_0^+ = 0$ and $\xi_L = \infty$. The integral equation becomes homogeneous

$$\beta(\xi) = \frac{1}{2}\int_0^\infty \beta(\xi_1)E_1(|\xi - \xi_1|)d\xi_1 \tag{17}$$

and the physical constants that should determine the magnitude of the emission function $\beta(\xi)$ seemingly disappear from the problem. Actually, the one constant that fixes the radiation level in this case is the constant value of flux. The function $\beta(\xi)$ must be related to q which means that equation (12) cannot be disregarded. Equation (12) is, in fact, the fundamental governing equation; the derivation leading to equation (16), or (17), involves the loss of a physical constant, and it might be expected that under the most general conditions a restoration of the constant would be required.

In astrophysics the study of a semi-infinite atmosphere under conditions involving thermodynamic equilibrium is referred to as Milne's restricted problem, and equation (17) is called the Milne (or Milne-Schwarzschild) integral equation. A more than substantial literature exists on the mathematical analysis of this particular idealization. Milne's equation is obviously a limiting case ($\xi_L \to \infty$, $q_0^+ \to 0$) of equation (16) and in this sense the highly accurate solutions in existence for the Milne problem can be used as a check on extreme conditions for the present study of radiation transport between parallel walls. Passage to the limit is not always direct, however.

GENERAL SOLUTION

Equation (16) is a Fredholm integral equation of the second kind. It takes the classical form

$$\beta(\xi) = f(\xi) + \frac{1}{2} \int_0^{\xi_L} \beta(\xi_1) E_1(|\xi - \xi_1|) d\xi_1 \tag{18}$$

where

$$2f(\xi) = q_0^+ E_2(\xi) + q_L^- E_2(\xi_L - \xi)$$

Much of the mathematical literature devoted to this type of problem is built around the use of the Schwarz inequality (see, e.g., Tricomi [7], p. 50 et seq.) which in turn leads to integration of the square of the kernel function. Rather than relate the analysis to general concepts, it is more expedient to derive what results are needed. The knowledge that the kernel $E_1(|\xi - \xi_1|)$ is everywhere positive will be used.

Let ξ_L be a finite constant. We prove first that the solution can be calculated by repeated iteration. The first $(n + 1)$ iterations in the calculation of $\beta(\xi)$ lead to the sequence $\beta_{n+1}(\xi)$ where

$$\beta_1(\xi) = f(\xi)$$

$$\beta_2(\xi) = f(\xi) + \frac{1}{2} \int_0^{\xi_L} f(\xi_1) E_1(|\xi - \xi_1|) d\xi_1 \tag{19}$$

$$\beta_{n+1}(\xi) = f(\xi) + \frac{1}{2}\int_0^{\xi_L} f(\xi_1)E_1(|\xi - \xi_1|)d\xi_1 + \ldots$$
$$+ \frac{1}{2^n}\int_0^{\xi_L} d\xi_n E_1(|\xi - \xi_n|)\int_0^{\xi_L} d\xi_{n-1}E_1(|\xi_n - \xi_{n-1}|) \ldots$$
$$\int_0^{\xi_L} d\xi_1 f(\xi_1)E_1(|\xi_2 - \xi_1|)$$

The relations

$$f(\xi) \leq f_{max} \tag{20a}$$

$$\left[\frac{1}{2}\int_0^{\xi_L} E_1(|\xi - \xi_1|)d\xi_1\right]_{max} = \frac{1}{2}\left[2 - E_2(\xi) - E_2(\xi_L - \xi)\right]_{max} \leq M < 1 \tag{20b}$$

apply for finite ξ_L. Then since the kernel is positive, repeated use of the mean value theorem for integrals yields

$$\beta_{n+1}(\xi) \leq f_{max}(1 + M + M^2 + \ldots + M^n) < \frac{f_{max}}{1 - M}$$

The sequence for positive terms therefore converges for all ξ.

For a nonunique solution to exist, a finite, nonvanishing solution of

$$\beta(\xi) = \frac{1}{2}\int_0^{\xi_L} \beta(\xi_1)E_1(|\xi - \xi_1|)d\xi_1 \tag{21}$$

would be required. Meghreblian [8] has shown that this is impossible as follows. From equations (20b) and (21), the inequality

$$|\beta(\xi)| \leq \frac{1}{2}\int_0^{\xi_L} |\beta(\xi_1)|E_1(|\xi - \xi_1|)d\xi_1 \leq M|\beta_{max}| < |\beta_{max}| \tag{22}$$

holds. But this cannot apply for <u>all</u> ξ in the range $0 \leq \xi \leq \xi_L$.

The finiteness of ξ_L is an important condition underlying the above results. Retaining this condition and returning to equation (16) one can show that

$$\beta\left(\frac{\xi_L}{2}\right) = \frac{1}{2}\,(q_o^+ + q_L^-) \tag{23}$$

and that the function is antisymmetric about the point $\xi = \xi_L/2$. In fact, straightforward manipulation of equation (16) reveals that the function $\beta(\xi) + \beta(\xi_L - \xi) - (q_o^+ + q_L^-)$ satisfies the homogeneous form of the integral equation (eq. (21)). But for finite ξ_L we have noted that the solution must vanish throughout the range of integration and this establishes the antisymmetry property

$$\beta(\xi) - \frac{q_o^+ + q_L^-}{2} = \frac{q_o^+ + q_L^-}{2} - \beta(\xi_L - \xi) \tag{24}$$

When $\xi = \xi_L/2$, equation (23) is seen to hold.

In actual calculation and in the presentation of results it is convenient to introduce the function $\varphi(\xi)$, where

$$\varphi(\xi) = \frac{\beta(\xi)}{q_L^- - q_o^+} - \frac{q_o^+ + q_L^-}{2(q_L^- - q_o^+)} \tag{25}$$

From equations (23) and (24) one concludes that $\varphi(\xi_L/2) = 0$ and that $\varphi(\xi)$ is antisymmetric about the point $\xi = \xi_L/2$. The integral equation for $\varphi(\xi)$ is, from equations (16) and (25),

$$\varphi(\xi) = \frac{1}{4}\,[E_2(\xi_L - \xi) - E_2(\xi)] + \frac{1}{2}\int_0^{\xi_L} \varphi(\xi_1)E_1(|\xi - \xi_1|)d\xi_1 \tag{26}$$

The function $\varphi(\xi)$ has no explicit dependence on q_o^+ and q_L^-.

Calculation of Solution

The main objective of the analysis was to calculate the emission function $\beta(\xi)$, knowing the wall temperatures and radiative characteristics. Equation (25) shows that when $\beta(\xi)$ is made dimensionless by dividing by $q_L^- - q_o^+$, the problem separates into two calculations:

(a) Determination of the universal functions $\varphi(\xi)$ which depend on the single parameter ξ_L.

(b) Determination of $(q_o^+ + q_L^-)$ and $(q_L^- - q_o^+)$ which are constant for given conditions but which depend on all of the given parameters of the problem as well as the solution $\varphi(\xi)$.

Before the numerical solutions are presented, additional relations will be given to establish the interdependence between the various parameters. We assume here that ξ_L has been fixed and that the function $\varphi(\xi)$ has been calculated. Substitution from equation (25) into equations (14) then yields, after setting

$$\left.\begin{aligned} Z &= 1 - 4r_o r_L E_3{}^2(\xi_L) \\ A &= \frac{1}{2}\left[\frac{1}{2} - E_3(\xi_L)\right] \\ K_o(\xi_L) &= \int_0^{\xi_L} \varphi(\xi_1)E_2(\xi_1)d\xi_1 \end{aligned}\right\} \qquad (27)$$

the two simultaneous equations for q_o^+ and q_L^-

$$q_o^+ [Z + 2r_o(K_o - A) - 4r_o r_L E_3(\xi_L)(K_o + A)] + q_L^- [-2r_o(K_o + A) + 4r_o r_L E_3(\xi_L)(K_o - A)] = \epsilon_o \sigma T_o^4 + 2r_o E_3(\xi_L)\epsilon_L \sigma T_L^4 \tag{28a}$$

$$q_o^+ [-2r_L(K_o + A) + 4r_o r_L E_3(\xi_L)(K_o - A)] + q_L^- [Z + 2r_L(K_o - A) - 4r_o r_L E_3(\xi_L)(K_o + A)] = 2r_L E_3(\xi_L)\epsilon_o \sigma T_o^4 + \epsilon_L \sigma T_L^4 \tag{28b}$$

If the additional notation

$$\begin{aligned}\Delta &= Z + 2[(r_o + r_L)(K_o - A) - 4r_o r_L E_3(\xi_L)(K_o + A) - 8r_o r_L K_o A] \\ &= 1 - r_o r_L + (r_o + r_L - 2r_o r_L)\left[2K_o(\xi_L) + E_3(\xi_L) - \frac{1}{2}\right]\end{aligned} \tag{29}$$

is introduced, the determinant of the coefficients of the simultaneous equations is $Z \cdot \Delta$ and the solution of equations (28) yields

$$q_o^+ = \frac{1}{\Delta}\left\{\epsilon_o \sigma T_o^4[1 + 2r_L(K_o - A)] + 2r_o \epsilon_L \sigma T_L^4[E_3(\xi_L) + K_o + A]\right\} \tag{30a}$$

$$q_L^- = \frac{1}{\Delta}\left\{2r_L \epsilon_o \sigma T_o^4[E_3(\xi_L) + K_o + A] + \epsilon_L \sigma T_L^4[1 + 2r_o(K_o - A)]\right\} \tag{30b}$$

Thus

$$q_L^- - q_o^+ = \frac{1}{\Delta}[(1 - r_o)\epsilon_L \sigma T_L^4 - (1 - r_L)\epsilon_o \sigma T_o^4] \tag{31a}$$

$$q_L^- + q_o^+ = \frac{1}{\Delta}\left\{\epsilon_L \sigma T_L^4[(1 + r_o) + 4r_o(K_o - A)] + \epsilon_o \sigma T_o^4[(1 + r_L) + 4r_L(K_o - A)]\right\} \tag{31b}$$

From equations (12) and (25), at $\xi = 0$

$$q = (q_L^- - q_o^+)\left[-\frac{1}{2} - E_3(\xi_L) - 2K_o(\xi_L)\right] \tag{32a}$$

and at $\xi = \xi_L/2$

$$q = (q_L^- - q_o^+)\left[-2E_3\left(\frac{\xi_L}{2}\right) + 4K_1(\xi_L)\right] \tag{32b}$$

where

$$K_1(\xi_L) = \int_0^{\xi_L/2} \varphi(\xi_1)E_2\left(\frac{\xi_L}{2} - \xi_1\right) d\xi_1$$

Flux, q, and the emission function, $\beta(\xi)$, are finally expressed in terms of the universal function $\varphi(\xi)$, the boundary conditions involving σT_o^4, σT_L^4 and the wall parameters as follows:

$$\beta(\xi) = \frac{1}{\Delta}\Big\{[(1 - r_o)\epsilon_L\sigma T_L^4 - (1 - r_L)\epsilon_o\sigma T_o^4]\varphi(\xi) + \frac{1}{2}\epsilon_L\sigma T_L^4[(1 + r_o)$$

$$+ 4r_o(K_o - A)] + \frac{1}{2}\epsilon_o\sigma T_o^4[(1 + r_L) + 4r_L(K_o - A)]\Big\}$$

$$= \frac{1}{\Delta}\Big([(1 - r_o)\epsilon_L\sigma T_L^4 - (1 - r_L)\epsilon_o\sigma T_o^4]\varphi(\xi) + \frac{1}{2}\epsilon_L\sigma T_L^4\{1 + 2r_o[2K_o(\xi_L)$$

$$+ E_3(\xi_L)]\} + \frac{1}{2}\epsilon_o\sigma T_o^4\{1 + 2r_L[2K_o(\xi_L) + E_3(\xi_L)]\}\Big) \tag{33a}$$

$$q = \frac{-1}{2\Delta}[1 + 2E_3(\xi_L) + 4K_o(\xi_L)][(1 - r_o)\epsilon_L\sigma T_L^4 - (1 - r_L)\epsilon_o\sigma T_o^4]$$

$$= -\frac{2}{\Delta}\left[E_3\left(\frac{\xi_L}{2}\right) - 2K_1\right][(1 - r_o)\epsilon_L\sigma T_L^4 - (1 - r_L)\epsilon_o\sigma T_o^4] \tag{33b}$$

where A, K_o, K_1, and Δ are given in equations (27), (29), and (32).

The integral equation (26) for $\varphi(\xi)$ can be rewritten in an alternative form. From equations (12) and (32) this is

$$-\frac{1}{2} - E_3(\xi_L) + E_3(\xi) + E_3(\xi_L - \xi)$$
$$= 2\int_0^{\xi_L} \varphi(\xi_1)[\mathrm{sgn}(\xi - \xi_1)E_2(|\xi - \xi_1|) + E_2(\xi_1)]d\xi_1 \qquad (34)$$

Equation (26) can be rederived from equation (34) by taking the derivative of the latter with respect to ξ. Either equation is adaptable to the calculation of $\varphi(\xi)$ by numerical means. The first is a Fredholm equation of the second kind and, as shown previously, the proof of the convergence of iterative methods offers no analytic difficulty. Numerically, however, the singularity in the kernel at $\xi = \xi_1$ is an inconvenience requiring special attention. Equation (34) is a Fredholm equation of the first kind, is less well adapted to general analysis, but is numerically more tractable since the kernel is finite everywhere although it does possess a step discontinuity at $\xi = \xi_1$.

Equation (33a) shows that the variation of $\beta(\xi)$ depends essentially on the variation in $\varphi(\xi)$. For theoretical predictions, therefore, the basic calculations can be carried out for the case of opaque, black walls and for a given optical thickness ξ_L in order to fix $\varphi(\xi)$. Thus, the graphical results given by Usiskin and Sparrow [4] or by Meghreblian [8] can be used directly. The terminology used here differs from these references; it suffices merely to note, however, that $\varphi(\xi)$ is the deviation of the dimensionless emission function from its value optically midway between the walls. Following this determination, the exact level of the function $\beta(\xi)$ can be found after an additional integration to determine K_0 or K_0 and K_1. It will be shown in the next section that good approximations of the solutions can actually be carried out analytically. Graphical results will be given then.

APPROXIMATE SOLUTIONS

In this section, approximate solutions to the transfer equation are given in analytic form. First, the nature of $\varphi(\xi)$ will be determined when the kernel is arbitrarily replaced by an exponential function. This type of approximation is often used in more complex problems involving the coupling of radiative and other modes of energy transport (see, e.g., [9]). Situations like the present one, in which different orders of accuracy can be achieved, are of value in assessing the degree of accuracy that can be expected. Second, the exact kernel is retained but the analysis is restricted to the determination of a linearized form of $\varphi(\xi)$ together with its improvement by means of a single iteration. In general, this solution represents an improvement in accuracy over the first case but at some cost in ease of calculation. Third, a more refined process, representing a modified iteration of the exact equation, will be carried out. These latter results compare well with the previously published numerical solutions for $0 < \xi_L \leq 10$.

A commonly used approximation for $E_2(\xi)$ involves its replacement by an exponential function. More specifically, the relation

$$E_2(\xi) \approx me^{-n\xi} \tag{35}$$

is introduced where m and n are chosen in some plausible manner. A plot of the two functions shows that small deviations can be maintained throughout the full range of ξ, even though local discrepancies in the derivatives of the functions become excessive. This approximation was implicit in the early work of Eddington [10] on stellar atmospheres, the rationalization stemming from an averaging over the angular variable θ (or μ) of the integrals appearing in the derivation of the transport equations. Different values of m and n are found in the literature since compromises must be made when mean values of specific intensity, flux, and radiation pressure are required. A discussion from the point of view of the astrophysicist is given by Ambartsumian ([11], p. 17 et seq.). More recently, Vincenti and Baldwin [12] have proposed $m = n^2/3$, $n = 1.562$ which follow after the requirement is imposed that flux be given properly in the Rosseland limit of strong absorption and that equation (35) correspond to a least squares fit between the two functions. The first of these conditions is well founded physically and is common to all approximations. The second condition is obviously more arbitrary. Proposed values of n in the literature fall usually in the range $3/2 \leq n \leq \sqrt{3}$; the value 3/2, preferred by most authors, is the one associated with Eddington's approximation.

If the flux equation is written as

$$\frac{q}{q_L^- - q_o^+} = -[E_3(\xi) + E_3(\xi_L - \xi)] + 2\int_0^{\xi_L} \varphi(\xi_1)\operatorname{sgn}(\xi - \xi_1)E_2(|\xi - \xi_1|)d\xi_1 \tag{36}$$

the exponential approximation can be introduced in the integrand from equation (35). The resulting integral equation can be solved explicitly but the degree of approximation is affected only slightly and the analysis is made much simpler if the further approximation

$$E_3(\xi) = \int_{\xi}^{\infty} E_2(\xi_1)d\xi_1 \doteq \frac{m}{n} e^{-n\xi} = \frac{n}{3} e^{-n\xi} \tag{37}$$

is introduced. The integral equation then becomes

$$\frac{q}{q_L^- - q_o^+} = -\frac{m}{n}\left[e^{-n\xi} + e^{-n(\xi_L - \xi)}\right] + 2m\int_0^{\xi_L} \varphi(\xi_1)\,\mathrm{sgn}(\xi - \xi_1)e^{-n|\xi - \xi_1|}\,d\xi_1 \tag{38}$$

For constant flux, the solution is

$$\varphi(\xi) = \frac{n}{2 + n\xi_L}\left(\xi - \frac{\xi_L}{2}\right) \tag{39}$$

and consistent with the approximation used, one has

$$K_o = \frac{n}{6}\left(\frac{2 - n\xi_L}{2 + n\xi_L} - e^{-n\xi_L}\right); \qquad K_1 = \frac{n}{6}\left(-\frac{2}{2 + n\xi_L} + e^{-n\xi_L/2}\right)$$

For all values of the parameters the emission function $\beta(\xi)$ is therefore a linear function of ξ. From equations (31a) and (32b)

$$\frac{-q}{q_L^- - q_o^+} = \frac{4n}{3(2 + n\xi_L)} \tag{40a}$$

$$q_L^- - q_o^+ = \frac{(1 - r_o)\epsilon_L\sigma T_L^{\,4} - (1 - r_L)\epsilon_o\sigma T_o^{\,4}}{1 + (r_o + r_L)\left\{\dfrac{2[n - (3/2)] - n\xi_L[n + (3/2)]}{3(2 + n\xi_L)}\right\} - 2r_o r_L \dfrac{n}{3}\dfrac{2 - n\xi_L}{2 + n\xi_L}} \tag{40b}$$

At extreme values of ξ_L, flux is given by

$$\frac{-q}{q_L^- - q_o^+} \doteq \begin{cases} 1 \quad , & \xi_L \ll 1 \\ \frac{4}{3\xi_L} \quad , & \xi_L \gg 1 \end{cases} \tag{41}$$

When $n = 3/2$ and when the walls are opaque and black, equation (40a) is the interpolation formula for flux derived by Probstein by completely different methods. Probstein's graphical comparison of his formula and more accurate results indicated good agreement. Further comparisons, including different emissivities and reflectivities, will be given in figure 2.

Equations (41) give intuitively obvious results: for optically thin media ($\xi_L \ll 1$) flux is merely the difference between the total emissions from the two walls; for optically thick media, where the mean free path of the radiation is small, the flux is in agreement with the predictions of Rosseland's approximation. The Rosseland theory reduces the radiation transport equation to the heat conduction equation with an effective, nonlinear conductivity. For a gray material with unit index of refraction, flux is given by

$$q \approx -\frac{4}{3}\frac{d\beta}{d\xi} \tag{42}$$

Equation (42) holds only for $\xi_L \gg 1$ and boundary conditions are strictly applicable only to the case of opaque, black walls. Integration of equation (42) for constant q then leads directly to the second of equations (41).

An improved approximation can be achieved through a study of equation (26) directly. The function $\varphi(\xi)$ is known to be asymmetric about $\xi = \xi_L/2$. To a first order, therefore, it is proper to set $\varphi(\xi) = \lambda[\xi - (\xi_L/2)]$ and seek λ. Direct substitution may then be made into equation (26), or into the derivative of this relation, which has the form

$$\varphi'(\xi) = \frac{1}{4}[1 + 2\varphi(0)]E_1(\xi) + \frac{1}{4}[1 - 2\varphi(\xi_L)]E_1(\xi_L - \xi) + \frac{1}{2}\int_0^{\xi_L} \varphi'(\xi_1)E_1(|\xi - \xi_1|)d\xi_1 \tag{43}$$

The calculation gives, at $\xi = \xi_L/2$,

$$\lambda E_2\left(\frac{\xi_L}{2}\right) - \varphi(0)E_1\left(\frac{\xi_L}{2}\right) = \frac{E_1(\xi_L/2)}{2} \tag{44}$$

The linear approximation for φ yields $\varphi(0) = -\lambda\xi_L/2$. This latter expression, together with equation (44), gives the following predictions

$$\lambda = \frac{e^{\xi_L/2}E_1(\xi_L/2)}{2} \tag{45a}$$

$$\varphi(\xi) = \frac{e^{\xi_L/2}E_1(\xi_L/2)[\xi - (\xi_L/2)]}{2} \tag{45b}$$

$$\left.\begin{aligned} K_0 &= \lambda\left\{[E_4(0) - E_4(\xi_L)] - \frac{\xi_L}{2}[E_3(0) + E_3(\xi_L)]\right\} \\ K_1 &= \lambda\left\{\frac{\xi_L}{2}E_3\left(\frac{\xi_L}{2}\right) - \left[E_4(0) - E_4\left(\frac{\xi_L}{2}\right)\right]\right\}\end{aligned}\right\} \tag{45c}$$

$$\frac{-q}{q_L^- - q_o^+} = \frac{4}{3}\lambda\left[1 + 3\,\frac{E_2(\xi_L/2)E_3(\xi_L/2) - E_1(\xi_L/2)E_4(\xi_L/2)}{E_1(\xi_L/2)}\right] \qquad (45d)$$

$$\begin{aligned} q_L^- - q_o^+ = [(1 - r_o)\epsilon_L\sigma T_L^{\,4} - (1 - r_L)\epsilon_o\sigma T_o^{\,4}]\Bigg\{1 \\ + (r_o + r_L)\left[-\frac{1}{2} - \lambda\left(\frac{\xi_L}{2} - \frac{2}{3}\right) + (1 - \lambda\xi_L)E_3(\xi_L) - 2\lambda E_4(\xi_L)\right] \\ -2r_o r_L\left[-\lambda\left(\frac{\xi_L}{2} - \frac{2}{3}\right) + (1 - \lambda\xi_L)E_3(\xi_L) - 2\lambda E_4(\xi_L)\right]\Bigg\}^{-1} \qquad (45e) \end{aligned}$$

Equation (45a) is in agreement with the determination of slope given by Meghreblian [8] for black walls but equation (45d) does not conform to his result. The linear approximation of $\varphi(\xi)$ does not yield constant flux and a decision must be made concerning its evaluation. The flux at $\xi_L/2$, as given in equation (45d), gives much better accuracy than flux evaluated at the wall.

Equations (45b) and (45d) represent improvements over the simplifications inherent in equations (39) and (40). The degree of accuracy of equation (45b) is, of course, limited since the predicted emission is expressed as a linear function of ξ throughout its range. By virtue of the additional integration to get flux, however, equation (45d) should provide good estimates. One notes that for extremes in ξ_L, equation (45d) reduces to the predictions of equations (41), as indeed it should from physical considerations.

An improved expression for $\varphi(\xi)$ now follows by iteration when equation (45b) is used to evaluate the integral in equation (26). This process is much to be preferred, analytically, to the more general iterative scheme employed in equation (19) since the first estimate is closer to the exact solution. The process is, in fact, similar to the iterative use of the Milne-Eddington approximation ([2], p. 87) to achieve a solution of the Milne equation.

Continued iteration beyond this stage is more difficult. A simpler process is available, however, in which integration of products of the transcendental functions is avoided while the accuracy is increased. To this end, in view of the known antisymmetry about $\xi = \xi_L/2$, we add a cubic term to the linear expression for $\varphi(\xi)$. Thus, we put

$$\varphi(\xi) = \lambda\left(\xi - \frac{\xi_L}{2}\right) + \gamma\left(\xi - \frac{\xi_L}{2}\right)^3 \tag{46}$$

where the slope λ at $\xi = \xi_L/2$ is given by (45a). A first approximation is found by inserting the linear form (45b) in the integral equation (26) to find

$$\begin{aligned}\varphi^{(1)}(\xi) &= \frac{1}{4}\left[E_2(\xi_L - \xi) - E_2(\xi)\right] + \frac{1}{2}\lambda\int_0^{\xi_L}\left(\xi_1 - \frac{\xi_L}{2}\right)E_1(|\xi - \xi_1|)d\xi_1 \\ &= \lambda\left(\xi - \frac{\xi_L}{2}\right) + \frac{1}{4}(1 - \lambda\xi_L)\left[E_2(\xi_L - \xi) - E_2(\xi)\right] + \frac{\lambda}{2}\left[E_3(\xi) - E_3(\xi_L - \xi)\right]\end{aligned} \tag{47}$$

A value for γ is determined by equating expressions (46) and (47), evaluated at $\xi = 0$;

$$\gamma^{(1)} = -\left(\frac{2}{\xi_L}\right)^3\left[\varphi^{(1)}(0) + \frac{1}{2}\lambda\xi_L\right]$$

Now put

$$\bar{\varphi}^{(2)}(\xi) = \lambda\left(\xi - \frac{\xi_L}{2}\right) + \gamma^{(1)}\left(\xi - \frac{\xi_L}{2}\right)^3$$

in the integral equation (26) and find

$$\varphi^{(2)}(\xi) = \frac{1}{4}\left[E_2(\xi_L - \xi) - E_2(\xi)\right] + \frac{1}{2}\int_0^{\xi_L} \bar{\varphi}^{(2)}(\xi_1)E_1(|\xi - \xi_1|)d\xi_1 \tag{48a}$$

There results from this integration

$$\varphi^{(2)}(\xi) = \varphi^{(1)}(\xi) + \frac{1}{2}\gamma^{(1)}H(\xi,\xi_L) \tag{48b}$$

where

$$\begin{aligned} H(\xi,\xi_L) &= \int_0^{\xi_L}\left(\xi_1 - \frac{\xi_L}{2}\right)^3 E_1(|\xi - \xi_1|)d\xi_1 \\ &= 2\left(\xi - \frac{\xi_L}{2}\right)^3 + 4\left(\xi - \frac{\xi_L}{2}\right) + \left(\frac{\xi_L}{2}\right)^3\left[E_2(\xi) - E_2(\xi_L - \xi)\right] \\ &\quad + 3\left(\frac{\xi_L}{2}\right)^2\left[E_3(\xi) - E_3(\xi_L - \xi)\right] + 3\xi_L\left[E_4(\xi) - E_4(\xi_L - \xi)\right] \\ &\quad + 6\left[E_5(\xi) - E_5(\xi_L - \xi)\right] \end{aligned}$$

This process can be repeated by setting up the scheme

$$\left.\begin{aligned}
\overline{\varphi}^{(3)}(\xi) &= \lambda\left(\xi - \frac{\xi_L}{2}\right) + \gamma^{(2)}\left(\xi - \frac{\xi_L}{2}\right)^3 \\
\gamma^{(2)} &= -\left(\frac{2}{\xi_L}\right)^3\left[\varphi^{(2)}(0) + \frac{1}{2}\lambda\xi_L\right] \\
\varphi^{(3)}(\xi) &= \varphi^{(1)}(\xi) + \frac{1}{2}\gamma^{(2)}H(\xi,\xi_L) \\
&\cdots\cdots\cdots\cdots\cdots\cdots \\
\overline{\varphi}^{(n)}(\xi) &= \lambda\left(\xi - \frac{\xi_L}{2}\right) + \gamma^{(n-1)}\left(\xi - \frac{\xi_L}{2}\right)^3 \\
\gamma^{(n-1)} &= -\left(\frac{2}{\xi_L}\right)^3\left[\varphi^{(n-1)}(0) + \frac{1}{2}\lambda\xi_L\right] \\
\varphi^{(n)}(\xi) &= \varphi^{(1)}(\xi) + \frac{1}{2}\gamma^{(n-1)}H(\xi,\xi_L)
\end{aligned}\right\} \quad (49)$$

and increasing n until successive results agree to the desired number of figures.

When a solution for $\varphi(\xi)$ has been obtained having the required accuracy, the quantities $q/(q_L^- - q_O^+)$, K_O, K_1 can be calculated according to their definitions in equations (27) and (32). For this purpose, it was thought to be sufficiently accurate to use the cubic expression

$$\overline{\varphi}^{(n)}(\xi) = \lambda\left(\xi - \frac{\xi_L}{2}\right) + \gamma^{(n-1)}\left(\xi - \frac{\xi_L}{2}\right)^3$$

and evaluate the integrals analytically, rather than to perform a numerical integration using $\varphi^{(n)}(\xi)$. The results are, using superscripts to indicate correspondence with the iterates shown in equations (49):

$$K_0^{(n)}(\xi_L) = \int_0^{\xi_L} \left[\lambda\left(\xi_1 - \frac{\xi_L}{2}\right) + \gamma^{(n-1)}\left(\xi_1 - \frac{\xi_L}{2}\right)^3\right] E_2(\xi_1)d\xi_1$$

$$= \lambda\left\{-\frac{1}{2}\xi_L[E_3(0) + E_3(\xi_L)] + [E_4(0) - E_4(\xi_L)]\right\}$$

$$+ \gamma^{(n-1)}\left\{-\left(\frac{\xi_L}{2}\right)^3[E_3(0) + E_3(\xi_L)] + 3\left(\frac{\xi_L}{2}\right)^2[E_4(0) - E_4(\xi_L)]\right.$$

$$\left. - 6\left(\frac{\xi_L}{2}\right)[E_5(0) + E_5(\xi_L)] + 6[E_6(0) - E_6(\xi_L)]\right\} \qquad (50a)$$

$$K_1^{(n)}(\xi_L) = \lambda\left\{\frac{\xi_L}{2}E_3\left(\frac{\xi_L}{2}\right) - \left[E_4(0) - E_4\left(\frac{\xi_L}{2}\right)\right]\right\}$$

$$+ \gamma^{(n-1)}\left\{\left(\frac{\xi_L}{2}\right)^3 E_3\left(\frac{\xi_L}{2}\right) + 3\left(\frac{\xi_L}{2}\right)^2 E_4\left(\frac{\xi_L}{2}\right)\right.$$

$$\left. + 6\left(\frac{\xi_L}{2}\right)E_5\left(\frac{\xi_L}{2}\right) - 6\left[E_6(0) - E_6\left(\frac{\xi_L}{2}\right)\right]\right\} \qquad (50b)$$

Once K_0 or K_1 is known, the flux follows from (32a) or (32b). Finally, numerical values for the quantity $(q_L^- - q_0^+)$ can be found by using the expression (50a) for K_0 for the calculation of Δ according to (29) and then using equation (31a).

PRESENTATION AND DISCUSSION OF RESULTS

In this section the analytic solutions previously derived will be shown graphically and some formulas of special interest will be given. Attention is directed first to flux since reasonable accuracy is not difficult to achieve.

The ratio $q/(q_L^- - q_o^+)$ does not distinguish between black-wall emission and the more general case. Hence, the two formulas, equations (40a) and (45d), can be compared directly with the numerical solution for black walls in [4] and [8] and also with a recent exact calculation of Hottel [13]. Figure 2 shows our predictions. The solid curve gives results from the iterative use of the cubic approximation to $\varphi(\xi)$ as outlined following equation (46). Through the range $0 \leq \xi_L \leq 2$ there is excellent agreement with published results and the solid curve appears to be a valid criterion to judge the merit of our other approximations. Unfortunately, discernible differences from the references can be detected in the range $3 \leq \xi_L \leq 10$ but comparable differences also exist between the references themselves. Since there is complete agreement at $\xi_L = 2$ and little doubt as to the approximation at $\xi_L = 10$, the slight deviations in the intermediate values are possibly attributable to the draftmanship of the published curves. The practical consequences are slight, however, and the present results appear valid to about two digit accuracy. The short-dash curve is equation (40a) (for $n = 3/2$) and is the interpolation formula proposed by Probstein [6]. Equation (45d) supplies another interpolation formula which affords a better fit on the lower end of the ξ_L scale but at a sacrifice of algebraic simplicity. In the range $2 \leq \xi_L \leq 6$ the interpolation formulas yield about the same accuracy but differ in the sign of the error. For $\xi_L \gg 1$ all results coalesce.

The next objective is to relate the magnitude of $q_L^- - q_O^+$ to the wall boundary conditions for the general case of nonblack walls. Equations (40b) and (45e) supply this information for the two linear forms of the emission function. Considerable simplification is achieved, however, if the walls are opaque or if they are alike in material properties. First, we shall restrict attention to opaque walls where $1 - r_O = \epsilon_O$, $1 - r_L = \epsilon_L$. From equations (29), (31a), and (32) one gets

$$\frac{q_L^- - q_O^+}{\sigma T_L{}^4 - \sigma T_O{}^4} = \frac{1}{1 + [-q/(q_L^- - q_O^+)][(1/\epsilon_O) + (1/\epsilon_L) - 2]} \tag{51}$$

Substitution into the denominator of the right member, from equations (40a) or (45d), provides the desired expression. For example, equation (40a) with $n = 3/2$ yields

$$\frac{q_L^- - q_O^+}{\sigma T_L{}^4 - \sigma T_O{}^4} = \frac{1 + 3\xi_L/4}{3\xi_L/4 + [(1/\epsilon_O) + (1/\epsilon_L) - 1]} \tag{52}$$

For large and small ξ_L equation (52) reduces to more familiar relations.

Figures 3 show, for opaque walls, the function $q/(\sigma T_L{}^4 - \sigma T_O{}^4)$ as given by the different approximations. The solid curves are presumably exact to the accuracy with which they can be read. The short-dash curves are, in effect, generalizations of Probstein's interpolation formula and, from equations (40a) and (52), are given by the relation

$$\frac{-q}{\sigma T_L{}^4 - \sigma T_O{}^4} = \frac{1}{3\xi_L/4 + [(1/\epsilon_O) + (1/\epsilon_L) - 1]} \tag{53}$$

The remaining curves (long dash) result from use of expression (45d) in equation (51). The dashed curves are not shown in all cases; differences from the solid curve can be estimated from the results shown, and the fact that the three approximations are indistinguishable for the lowest curve on each graph.

The relative merits of the simplest approximation, that is, the one associated with the exponential kernel, appear now to have been fully established insofar as predictions of flux are concerned. We therefore write, finally, the most general formula based upon this approach:

$$-q\bigg/\left[\frac{\epsilon_L \sigma T_L^{\;4}}{(1 - r_L)} - \frac{\epsilon_o \sigma T_o^{\;4}}{(1 - r_o)}\right] = 1\bigg/\left\{\frac{3}{4}\,\xi_L + \left[\frac{1}{(1 - r_L)} + \frac{1}{(1 - r_o)} - 1\right]\right\} \tag{54}$$

Equation (54) embraces and extends the previous interpolation formulas.

The actual distribution of emission, or of $\varphi(\xi)$, provides the most exacting demands upon the approximations underlying the predictions. In figure 4 the curves were calculated by two methods. The solid lines again correspond to repeated iteration of the cubic expression; the other curves are given by equation (47), the first iteration of the linear relation. No attempt was made to include the linear distributions of $\varphi(\xi)$ predicted by the simpler methods. To the scale of these figures both linear distributions conform to the straight lines tangent to $\varphi(\xi)$ at $\xi = \xi_L/2$. The standard of comparison comes from the numerical results plotted in [4] and [8]. It does not seem possible, because of inconsistencies in the published figures, to draw unequivocal conclusions about the accuracy. Qualitatively, the results may certainly be termed satisfactory but small local deviations exist in each case. These discrepancies are at most of the order of 1 or 2 percent. Diminishing preciseness inevitably occurs in the vicinity of the walls.

In figure 5 the dependence of the functions K_0, K_1, and A on ξ_L is shown according to the best approximations of this paper. These values are of use in further specific calculations of $\varphi(\xi)$ and in the determination of the level of the emission function.

In the initial part of this paper the analysis is cast in a general form and the problem of radiative transport between walls with rather arbitrary characteristics is related to the calculations involving black walls. In the latter part of the paper the philosophy is more one of pragmatism; namely, that to the accuracy of the physical idealization and to the accuracy of many engineering estimates, it is preferable to retain some analytic control over the results. In particular, the use of the simplifying assumptions leading to the use of the exponential kernel yields simple formulas of practical interest. Analytic methods are shown also to produce solutions of reasonable accuracy. The mathematical nature of the problem of radiative transport is of considerable interest to theorists, and, in the ultimate degree of perfection, numerical calculations appear to be required. Such methods are essential in fixing a standard of excellence and need to be understood if restrictions are to be relaxed and estimates of the effects of frequency-dependent absorptivity and emissivity are to be studied. On the other hand, a good grasp of the qualitative character of the solution is important in the extension to less idealized cases and algebraic formulas may be preferable to purely numerical results in filling this need.

REFERENCES

1. S. Chandrasekhar, Radiative Transfer. Oxford Univ. Press, N. Y. (1950). Also Dover Pub., Inc. (1960).

2. V. Kourganoff, Basic Methods in Transfer Problems. Oxford, Clarendon Press (1952).

3. V. V. Sobolev, A Treatise on Radiative Transfer. D. Van Nostrand (1963).

4. C. M. Usiskin, and E. M. Sparrow, Thermal Radiation Between Parallel Plates Separated by an Absorbing-Emitting Nonisothermal Gas. Int. J. Heat Mass Transfer, vol. 1, no. 1, pp. 28-36 (1960).

5. R. Goulard, and M. Goulard, One-Dimensional Energy Transfer in Radiant Media. Int. J. Heat Mass Transfer, vol. 1, no. 1, pp. 81-91 (1960).

6. Ronald F. Probstein, Radiation Slip. AIAA Jour., vol. 1, no. 5, pp. 1202-1204 (1963).

7. F. G. Tricomi, Integral Equations. Interscience Publishers, N. Y. (1957).

8. Robert V. Meghreblian, Radiation Exchange Between Two Flat Surfaces Separated by An Absorbing Gas. Tech. Rep. 32-197, Jet Prop Lab. (1962).

9. Max. A. Heaslet, and Barrett S. Baldwin, Predictions of the Structure of Radiation-Resisted Shock Waves. Phys. of Fluids, vol. 6, pp. 781-791 (1963).

10. A. S. Eddington, The Internal Constitution of the Stars. Cambridge University Press (1926). Also Dover Pub., N. Y. (1959).

11. V. A. Ambartsumian, ed., Theoretical Astrophysics. Pergamon Press, N. Y. (1958).

12. Walter G. Vincenti, and Barrett S. Baldwin, Jr., Effect of Thermal Radiation on the Propagation of Plane Acoustic Waves. Jour. Fluid Mech., vol. 12, pt. 3, pp. 449-477 (1962).

13. H. C. Hottel, Radiation as a Diffusion Process. Int. J. Heat Mass Transfer, vol. 5, pp. 82-83 (1962).

FIGURE LEGENDS

Figure 1.- Sketch showing parallel walls separated by absorbing medium.

Figure 2.- Dimensionless flux, as calculated by three methods of approximation, showing dependence on optical thickness.

Figure 3.- Dimensionless flux between opaque walls, showing dependence on optical thickness and wall emissivities.

Figure 4.- Approximations of universal function $\varphi(\xi/\xi_L)$ for different optical thicknesses.

Figure 5.- The functions $K_0(\xi_L)$, $K_1(\xi_L)$, and $A(\xi_L)$.

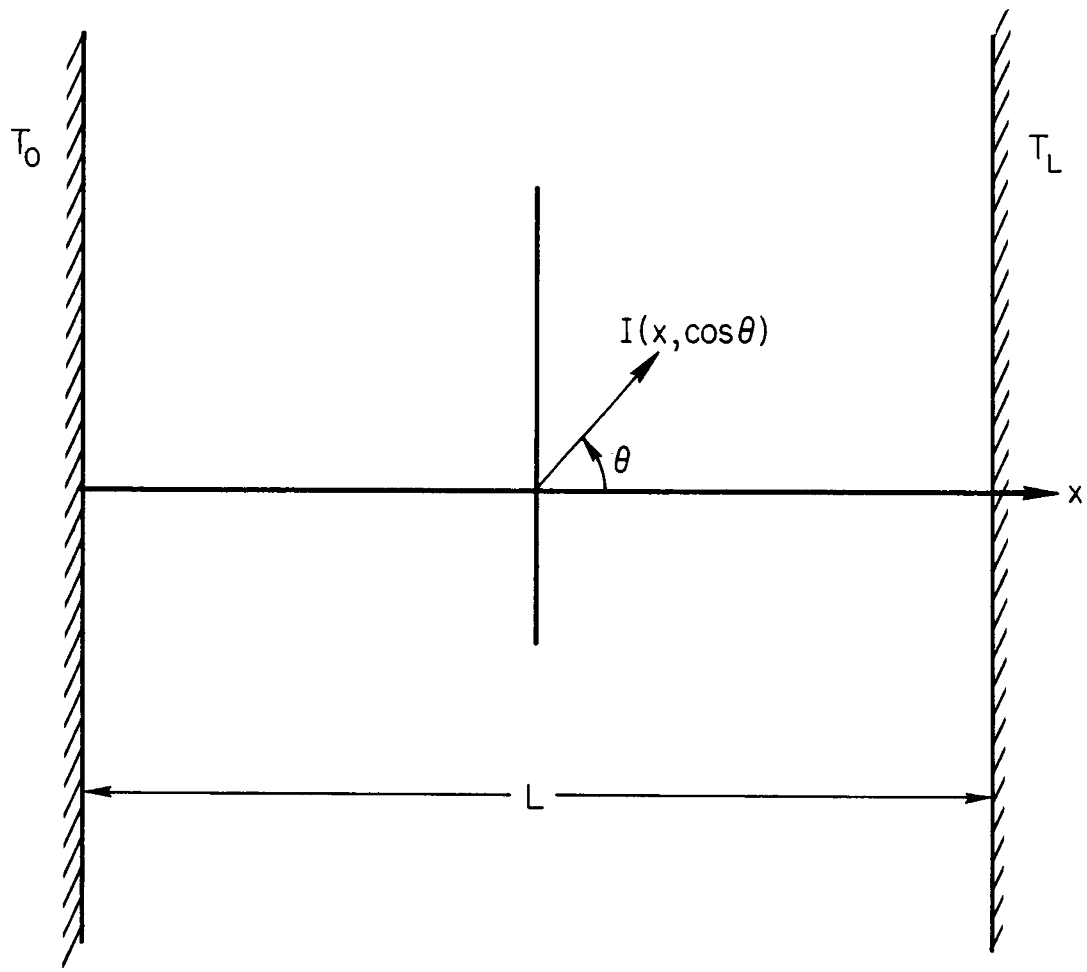

Figure 1.

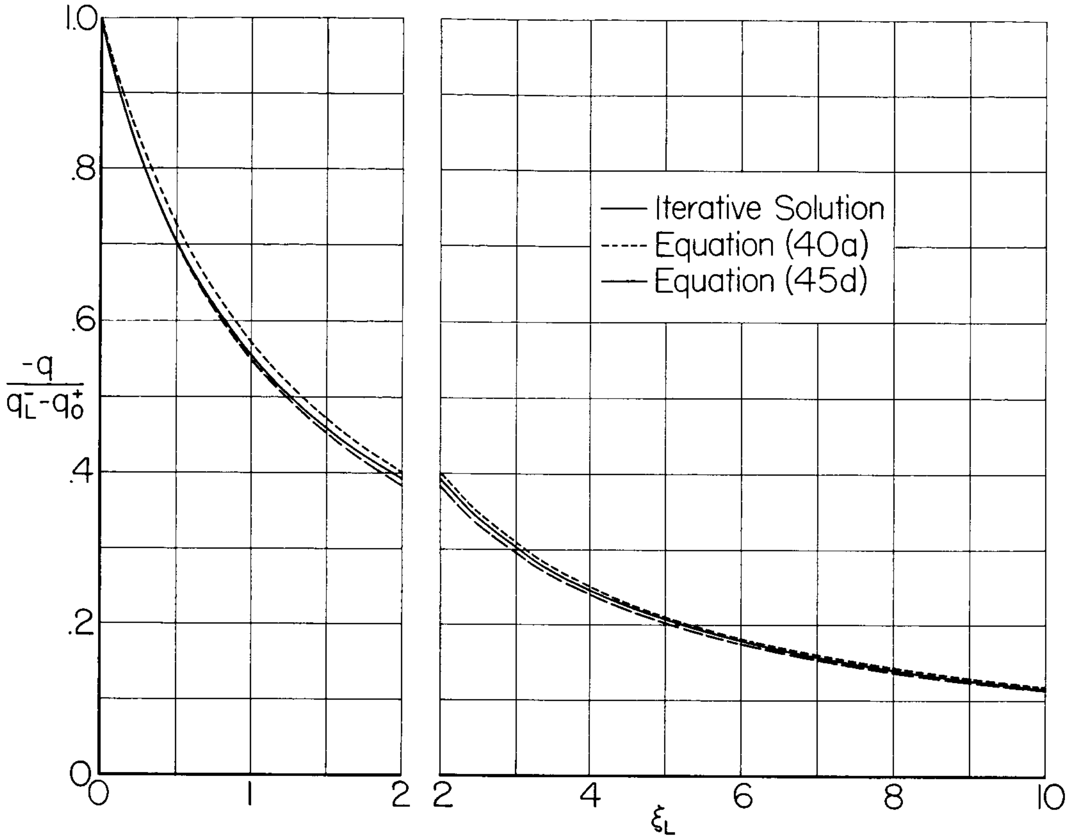
1.0
.8
.6
.4
.2
0
$\frac{-q}{q_L^- - q_0^+}$
0
1
2
2
4
6
8
10
ξ_L
Iterative Solution
Equation (40a)
Equation (45d)

Figure 2.

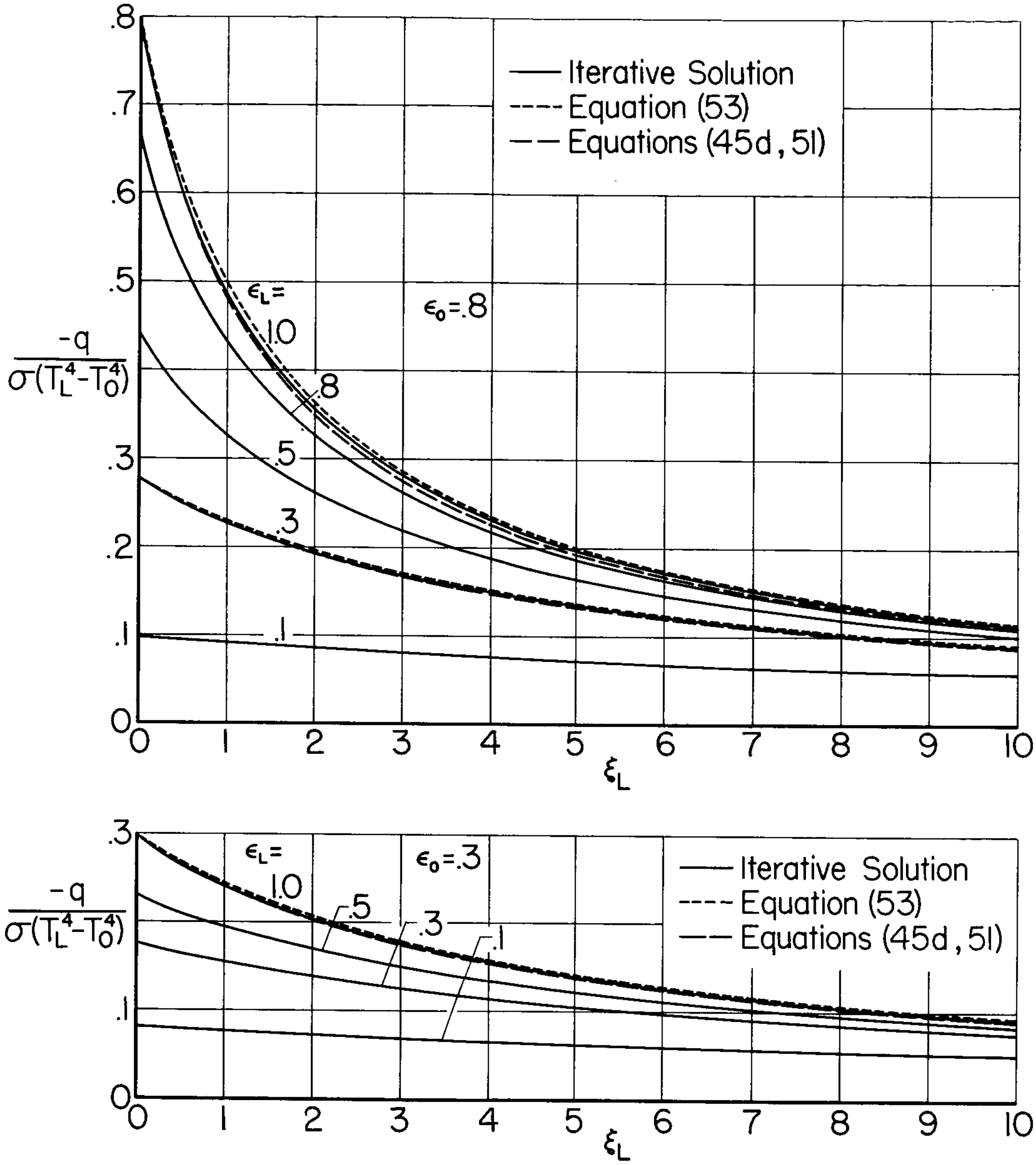

Figure 3.

NATIONAL AERONAUTICS AND SPACE ADMINISTRATION
AMES RESEARCH CENTER, MOFFETT FIELD, CALIFORNIA

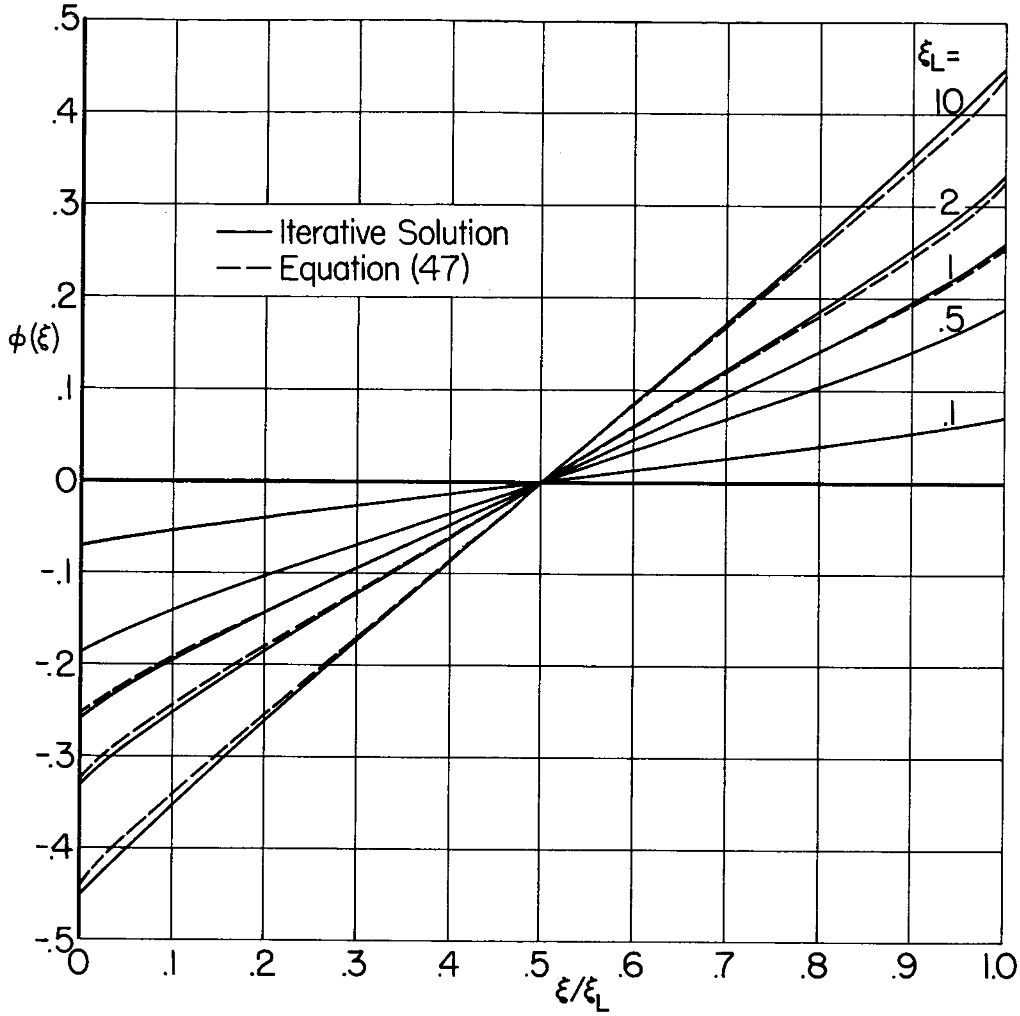

Figure 4.

NATIONAL AERONAUTICS AND SPACE ADMINISTRATION
AMES RESEARCH CENTER, MOFFETT FIELD, CALIFORNIA

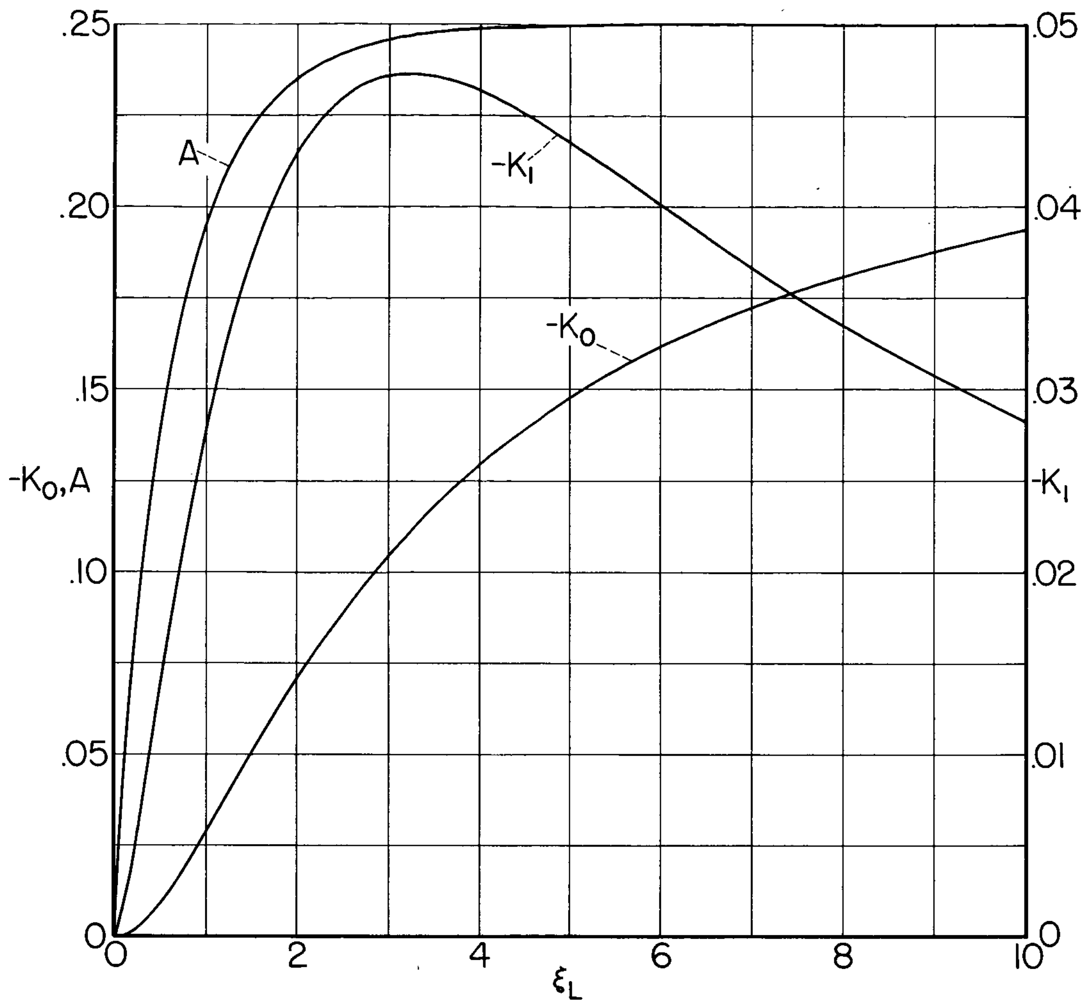

Figure 5.

NATIONAL AERONAUTICS AND SPACE ADMINISTRATION
AMES RESEARCH CENTER, MOFFETT FIELD, CALIFORNIA